

Electrostatic Docking of a Supramolecular Host–Guest Assembly to Cytochrome *c* Probed by Bidirectional Photoinduced Electron Transfer

Katarzyna I. Jankowska,[†] Cynthia V. Pagba,^{†,‡} Eugene L. Piatnitski Chekler,[§] Kurt Deshayes,^{||} and Piotr Piotrowiak^{*,†}

Department of Chemistry, Rutgers University, 73 Warren Street, Newark, New Jersey 07102, United States, Pfizer Inc., 257 East Point Road, Groton, Connecticut 06340, United States, and Genentech Inc., Department of Protein Engineering, 1 DNA Way, South San Francisco, California 94080, United States

Received March 15, 2010; E-mail: piotr@andromeda.rutgers.edu

Abstract: A water-soluble octacarboxyhemicarcerand was used as a shuttle to transport redox-active substrates across the aqueous medium and deliver them to the target protein. The results show that weak multivalent interactions and conformational flexibility can be exploited to reversibly bind complex supramolecular assemblies to biological molecules. Hydrophobic electron donors and acceptors were encapsulated within the hemicarcerand, and photoinduced electron transfer (ET) between the Zn-substituted cytochrome *c* (MW = 12.3 kD) and the host–guest complexes (MW = 2.2 kD) was used to probe the association between the negatively charged hemicarceplex and the positively charged protein. The behavior of the resulting ternary protein–hemicarcerand–guest assembly was investigated in two binding limits: (1) when $K_{\text{encaps}} \gg K_{\text{assoc}}$, the hemicarcerand transports the ligand to the protein while protecting it from the aqueous medium; and (2) when $K_{\text{assoc}} > K_{\text{encaps}}$, the hemicarcerand–protein complex is formed first, and the hemicarcerand acts as an artificial receptor site that intercepts ligands from solution and positions them close to the active site of the metalloenzyme. In both cases, ET mediated by the protein-bound hemicarcerand is much faster than that due to diffusional encounters with the respective free donor or acceptor in solution. The measured ET rates suggest that the dominant binding region of the host–guest complex on the surface of the protein is consistent with the docking area of the native redox partner of cytochrome *c*. The strong association with the protein is attributed to the flexible conformation and adaptable charge distribution of the hemicarcerand, which allow for surface-matching with the cytochrome.

Introduction

The concept of incarcerating small molecules into larger container compounds was introduced by Cram's group in the early 1980s.^{1,2} They synthesized the first carcerand, in the interior of which organic molecules were trapped as permanent guests.³ A few years later, the same group reported a new class of container molecules called hemicarcerands, which are capable of reversibly complexing guest compounds⁴ and releasing them upon thermal activation, irradiation,⁵ or under chemical stimulus. Hemicarcerands are closed-shell fully encapsulating hosts.⁶ They consist of two bowl-shaped units (cavitands) connected together by linking groups. The length of the linkers determines the

dimensions of cavity of the hemicarcerand and hence the maximum size of the guest that can be trapped inside.^{7,8} The linkers can be tailored to endow the hemicarcerand with the desired properties, for example, solubility in a particular medium or photolability. When guests become imprisoned inside these molecular capsules, complexes called hemicarceplexes are formed. They are stabilized by “intrinsic” and “constrictive” binding energy.^{9,10} Intrinsic binding energy is the standard free energy difference due to the encapsulation within the host's cavity. It consists of both attractive and repulsive interactions between the host and the guest, as well as of the changes in the solvation energy of both partners. Depending on the balance of these interactions, its overall value can be negative or positive. Constrictive binding energy is the energy barrier associated with the exit of the guest. If the barrier is much higher than $k_B T$, the

[†] Rutgers University.

[‡] Current address: Center for Biophotonics (CBST), Sacramento, CA 95817.

[§] Pfizer Inc.

^{||} Genentech Inc.

(1) Cram, D. J.; Cram, J. M. *Science* **1974**, *183*, 803–809.

(2) Cram, D. J. *Science* **1988**, *240*, 760–767.

(3) Cram, D. J.; Karbach, S.; Kim, Y. H.; Baczynskyj, L.; Marti, K.; Sampson, R. M.; Kallemeyn, G. W. *J. Am. Chem. Soc.* **1988**, *110*, 2554–2560.

(4) Quan, M. L. C.; Cram, D. J. *J. Am. Chem. Soc.* **1991**, *113*, 2754–2755.

(5) Piatnitski, E. L.; Deshayes, K. *Angew. Chem., Int. Ed.* **1998**, *37*, 970–972.

(6) Cram, D. J., Cram, J. M. *Container Molecules and Their Guests*; Monographs in Supramolecular Chemistry, Vol. 4; Stoddart, J. F., Series Ed.; RSC: Cambridge, 1994; pp 149–216, and references therein.

(7) Helgeson, R. C.; Peak, K.; Knobler, C. B.; Maverick, E. F.; Cram, D. J. *J. Am. Chem. Soc.* **1996**, *118*, 5590–5604.

(8) Cram, D. J.; Jaeger, R.; Deshayes, K. *J. Am. Chem. Soc.* **1993**, *115*, 1011–10116.

(9) Jasat, A.; Sherman, J. C. *Chem. Rev.* **1999**, *99*, 931–967.

(10) Warmuth, R.; Yoon, J. *Acc. Chem. Res.* **2001**, *34*, 95–105.

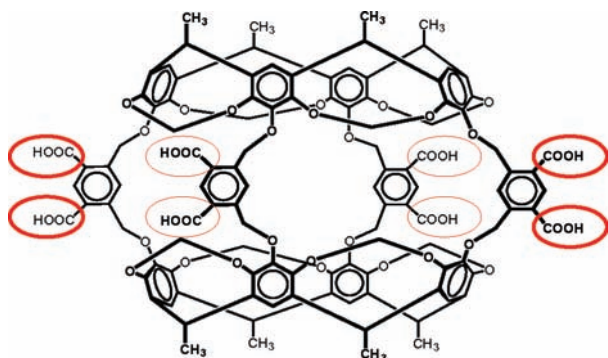


Figure 1. Cram-type water-soluble hemicarcerand used in this study. Note four 1,3-xylyleneoxy linkers flanking the “portals” of the hemicarcerand and eight carboxylic groups, which solubilize it in the aqueous medium, as well as enable the association with basic partners.

host–guest complex prepared at high temperature may persist for weeks and behave like a distinct, stable chemical species, even if the intrinsic binding energy is positive. Hemicarcerands offer much tighter binding than cyclodextrins with ΔG^0 values of ~ 10 versus ~ 4 kcal/mol,^{11,12} and far more complete protection of the guest from the external environment. They are the only carriers that can fully insulate small species such as the isotopes of I_2 , Xe, and Rn from contact with the biological medium. The size-selectivity of hemicarcerands is much higher than that of calixarenes or cyclodextrins. Many host molecules with diverse structures and applications were developed over the past decades. Nanoscale cages large enough to accommodate multiple guests¹³ and self-assembling hydrogen-bonded molecular capsules that enclose guest molecules in a reversible entropy-driven process were synthesized.¹⁴ Encapsulation was used both to stabilize short-lived intermediates^{15,16} as well as to accelerate the rates of chemical reactions and to control their regio- and stereoselectivity.^{17,18} Electron and energy transfer mediated by the walls of hemicarcerands of different size and composition were investigated in solution^{19–21} and at interfaces.²² More recently, the use of hemicarcerands in nanodevice fabrication²³ and in drug delivery²⁴ has been demonstrated.

In this Article, we present the application of a water-soluble octacarboxy–hemicarcerand²⁵ (Figure 1) as a molecular shuttle

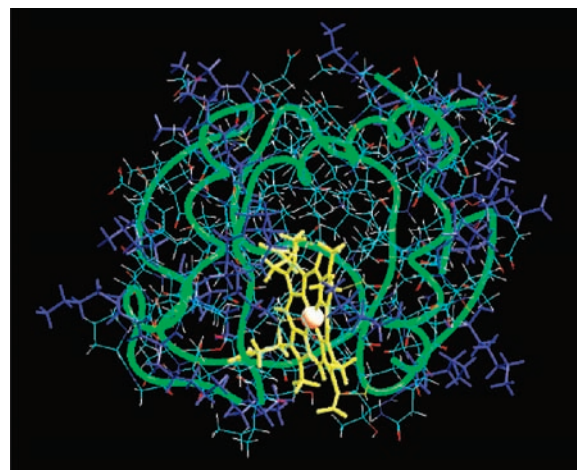


Figure 2. The X-ray structure of cytochrome *c* showing the basic lysine residues (blue) distributed on its surface and the heme pocket (PDB file: 1AKK).

capable of transporting small molecules across the aqueous medium and binding to the target biomolecule. The water-soluble hemicarcerand spontaneously encapsulates hydrophobic guests within its interior, with binding constants in the 10 nM to 100 μ M range. Cytochrome *c* was selected as the target protein because of its well-characterized structure,^{26,27} redox behavior,^{28–30} and the anticipated ability to reversibly associate with the octacarboxyhemicarcerand. The binding between the supramolecular host–guest assembly and its partner can rely on a variety of specific and nonspecific interactions. In the current system, we exploit the electrostatic interactions between the carboxylic groups of the hemicarcerand and the numerous basic residues (19 lysines and 2 arginines) present on the surface of cytochrome *c* (Figure 2). The isoelectric point of cytochrome *c* is 10, while the pK_a values of the *m*-phthalic acid “portals” of the hemicarcerand are 3.54 for the singly and 4.60 for the doubly deprotonated species, respectively. As a result, both partners can exist in a broad range of protonated and deprotonated states, and significant ionic association between the protein and the supramolecular cage can be expected at neutral and moderately basic pH values.

It is important to note the comparable dimensions of the cytochrome and the hemicarcerand. The effective radius of the former is 14.3 Å and of the latter is 7.8 Å. The charge density on the surface of cytochrome *c* is asymmetric, with a negative field surrounding a hydrophobic patch in the immediate vicinity of the active site.³¹ The basic areas localized in the closest neighborhood of the heme pocket were identified as binding sites for the natural redox partners of cytochrome *c*, including cytochrome *c* peroxidase, cytochrome *bc*₁ complex, and cytochrome oxidase.^{32–34} A different binding preference was

- (11) Tucker, E. E.; Christian, S. C. *J. Am. Chem. Soc.* **1984**, *106*, 1942–1945.
- (12) Schneider, H.-J.; Yatsimirski, A. *Principles and Methods in Supramolecular Chemistry*; Wiley & Sons: Chichester, 2000.
- (13) Liu, X.; Liu, Y.; Li, G.; Warmuth, R. *Angew. Chem., Int. Ed.* **2006**, *45*, 901–904.
- (14) Ajami, D.; Rebek, J., Jr. *Nat. Chem.* **2009**, *1*, 87–90.
- (15) Cram, D. J.; Tanner, M. E.; Thomas, R. *Angew. Chem., Int. Ed. Engl.* **1991**, *30*, 1024–1027.
- (16) Warmuth, R.; Makowiec, S. *J. Am. Chem. Soc.* **2007**, *129*, 1233–1241.
- (17) Kang, J.; Rebek, J., Jr. *Nature* **1997**, *385*, 50–52.
- (18) Warmuth, R.; Kerdelhué, J.-L.; Sánchez Carrera, S.; Langenwalter, K. J.; Brown, N. *Angew. Chem., Int. Ed.* **2002**, *41*, 96–99.
- (19) Piotrowiak, P. *Chem. Soc. Rev.* **1999**, *28*, 143–150.
- (20) Place, I.; Farran, A.; Deshayes, K.; Piotrowiak, P. *J. Am. Chem. Soc.* **1998**, *120*, 12626–12633.
- (21) Piotrowiak, P.; Deshayes, K.; Romanova, Z. S.; Pagba, C.; Hore, S.; Zordan, G.; Place, I.; Farrán, A. *Pure Appl. Chem.* **2003**, *75*, 1061–1068.
- (22) Romanova, Z. S.; Deshayes, K.; Piotrowiak, P. *J. Am. Chem. Soc.* **2001**, *123*, 11029–11036.
- (23) Menozzi, E.; Pinalli, R.; Speets, E. A.; Ravoo, B. J.; Dalcanale, E.; Reinhardt, D. N. *Chem.-Eur. J.* **2004**, *10*, 2199–2206.
- (24) Gibb, C. L. D.; Gibb, B. C. *J. Am. Chem. Soc.* **2004**, *126*, 1408–11409.
- (25) Yoon, J.; Cram, D. J. *Chem. Commun.* **1997**, 497–498.

- (26) Takano, T.; Kallai, O. B.; Swanson, R.; Dickerson, R. E. *J. Biol. Chem.* **1973**, *248*, 5234–5255.
- (27) Banci, L.; Bertini, I.; Gray, H. B.; Luchinat, C.; Reddig, T.; Rosato, A.; Turano, P. *Biochemistry* **1997**, *36*, 9867–9877.
- (28) Shaila Gupte, S.; Hackenbrock, C. R. *J. Biol. Chem.* **1988**, *263*, 5241–5247.
- (29) Pelletier, H.; Kraut, J. *Science* **1993**, *258*, 1748–1755.
- (30) Zhou, J. S.; Hoffman, B. M. *Science* **1994**, *265*, 1693–1696.
- (31) Koppenol, W. H.; Margoliash, E. *J. Biol. Chem.* **1982**, *257*, 4426–4437.
- (32) Guo, M.; Bhaskar, B.; Li, H.; Barrows, T. P.; Poulos, T. L. *Proc. Natl. Acad. Sci. U.S.A.* **2004**, *101*, 5940–5945.
- (33) Lange, C.; Hunte, C. *Proc. Natl. Acad. Sci. U.S.A.* **2002**, *99*, 2800–2805.

Table 1. Experimental Rates and Thermodynamic Parameters for the Electron Transfer Reaction between $^3\text{ZnCC}^*$ and Host–Guest Complexes as well as Free Donors and Acceptors in Solution

quencher	E_{ox} [V]	E_{red} [V]	$\Delta G_{\text{ET}}^{\circ}$ [eV] ⁱ	k_{ET} [s ⁻¹] ^j	ET direction
Fc@Cage	0.31 ^a		-0.09	8.9×10^2	reduction
Ru@Cage	0.69 ^a		0.29	7.0×10^1	reduction
DQ@Cage		-0.24 ^b	-0.66	1.1×10^5	oxidation
Naph@Cage	1.54 ^c	-2.49 ^c	1.14 (1.59) ^d		
Ada@Cage	2.72 ^e		2.32		
Fc(COOH) ₂	0.64 ^f		0.24	3.2×10^2	reduction
DQ		-0.24 ^b	-0.66	5.4×10^3	oxidation
CQ		0.65 ^g	-1.55	9.8×10^2	oxidation
BQ		0.08 ^g	-0.98	1.0×10^2	oxidation
Naph(COOH) ₄	1.54 ^h	-2.49 ^b	1.14 (1.59) ^d		

^a The values for free donors: Kuwana, T.; Bublitz, D. E.; Hoh, G. *J. Am. Chem. Soc.* **1960**, *82*, 5811–5817. ^b The value for free duroquinone: Meisel, D.; Czapski, G. *J. Phys. Chem.* **1975**, *79*, 1503–1509. ^c The value for free naphthalene: Murov, S. L.; Carmichael, I.; Hug, G. L. *Handbook of Photochemistry*, 2nd ed.; Dekker: New York, 1993. ^d Driving force for the reduction of naphthalene. ^e Oxidation potential of adamantane: Mella, M.; Freccero, M.; Soldi, T.; Fasani, E.; Albin, A. *J. Org. Chem.* **1996**, *61*, 1413–1422. ^f The value taken from: Quaranta, D.; McCarty, D. R.; Bandarian, V.; Rensing, C. *J. Bacteriol.*, **2007**, *189*, 5361–5371, corresponds to neutral Fc(COOH)₂. Under the pH conditions of our experiments, the compound is present as the easier to oxidize monoanion Fc(COOH)(COO⁻). ^g Siraki, A. G.; Chan, T. S.; O'Brien, P. J. *Toxicol. Sci.* **2004**, *81*, 148–159. ^h The values for unsubstituted naphthalene from footnote *c* were used. ⁱ The free energy change for the reaction of ZnCC with the quencher is given by: $\Delta G = E_{\text{ox(D)}} - E_{\text{red(A)}} - E_{0-0(\text{triplet})}$, where $E_{\text{ox(Zn/Zn}^+)} = 0.8$ V; $E_{\text{red(Zn/Zn}^-)} = -1.3$ V; $E_{0-0(\text{triplet})} = 1.7$ V (ref 47, *Inorg. Chem.* **1996**, *35*, 2780). ^j The quenching rate for ZnCC (1×10^{-6} M) in the presence of quencher at pH = 7; the quencher concentration for presented results was equal 1.0×10^{-4} M except for DQ, BQ, and CQ (1.5×10^{-4} M).

observed by Niki et al. who studied electron transfer in cytochrome *c* on carboxylate SAMs on gold.³⁵ It was shown by Jain et al. that surface ligands containing an appropriate combination of charge and hydrophobic groups associate to cytochrome *c* with higher affinity than the ligands, which colligate only through the same number of anionic groups.³⁶ Because of the large size of the hemicarcerplex, as well as the presence of hydrophobic areas on its surface, it can be expected that the association between the hemicarcerplex and the cytochrome will resemble more closely the multivalent interaction between two proteins, rather than the binding of a small ligand.

The hemicarcerplex–protein association was monitored by photoinduced electron transfer between the encapsulated guest and Zn-substituted cytochrome *c* (ZnCC). The heme unit of native cytochrome *c* can act as an effective quencher in electron and excitation transfer experiments; however, due to its extremely short excited state lifetime (50 fs or less),³⁷ it is not a useful light absorbing chromophore. For this reason, Zn–Fe substitution has been used frequently in electron transfer studies on heme proteins.^{38–40} Zn–cytochrome *c* has a long-lived emissive triplet excited state, whose lifetime varies from 7 to 15 ms depending on the preparation and experimental conditions.^{41–43} Furthermore, the $^3\text{ZnCC}^*$ triplet is easily oxidized and reduced.^{44–47} Therefore, it can act both as an electron donor in

ET reactions with strong acceptors (quinones, nitro-aromatics) and as an acceptor with easily oxidized donors (ferrocene, aryl amines). The guests used in our study (Table 1) were selected on the basis of size and redox activity: ferrocene and ruthenocene are good electron donors, and their molecular volume of $\sim 180 \text{ \AA}^3$ is close to the maximum that can be accommodated within the cavity of the hemicarcerand ($\sim 200 \text{ \AA}^3$), duroquinone ($\sim 181 \text{ \AA}^3$) is a potent electron acceptor, while naphthalene ($\sim 151 \text{ \AA}^3$) and adamantane ($\sim 159 \text{ \AA}^3$), which cannot undergo electron transfer with $^3\text{ZnCC}^*$, served as the reference redox-inactive guests. Both singlet and triplet energy transfer from ZnCC* to any of the selected guests are endothermic by at least 0.7 eV. As a result, any observed emission quenching can be unambiguously attributed to electron transfer. To better understand the association of the hemicarcerplex with the cytochrome and its role in mediating the electron transfer reaction, control experiments on $^3\text{ZnCC}^*$ in the presence of free ferrocenedicarboxylic acid, as well as sparingly water-soluble quinones and the redox inactive carboxynaphthalenes, were performed. Electron transfer quenching of $^3\text{ZnCC}^*$ by the protein-bound host–guest complex was in all cases much faster than for the corresponding free donors and acceptors in solution. While other hosts such as cyclodextrins or cavitands have been used in conjunction with biomolecules in the past,^{48–50} the application of a fully encapsulating hemicarcerand to deliver both oxidizing and reducing partners to a redox-active protein has not been demonstrated before.

Materials and Methods

The general approach used in these studies is presented in Figure 3. First, the selected guest was encapsulated inside the hemicarcerand at room temperature and equilibrated. Next, the desired

- (34) Maneg, O.; Malatesta, F.; Ludwig, B.; Drosou, V. *Biochim. Biophys. Acta* **2004**, *1655*, 274–281.
 (35) Niki, K.; Pressler, K. R.; Sprinkle, J. R.; Li, H.; Margoliash, E. *Russ. J. Electrochem.* **2002**, *38*, 63–67.
 (36) Jain, R. K.; Tsou, L. K.; Hamilton, A. D. *Macrocyclic Chemistry: Current Trends and Future Perspectives*; Springer: New York, 2005; pp 267–275.
 (37) Franzen, S.; Kiger, L.; Poyart, C.; Martin, J.-L. *Biophys. J.* **2001**, *80*, 2372–2385.
 (38) Papp, S.; Vanderkooi, J. M.; Owen, C. S.; Holtom, G. R.; Phillips, C. M. *Biophys. J.* **1990**, *58*, 177–186.
 (39) Furukawa, Y.; Matsuda, F.; Ishimori, K.; Morishima, I. *J. Am. Chem. Soc.* **2002**, *124*, 4008–4019.
 (40) Horie, T.; Maniara, G.; Vanderkooi, J. M. *FEBS Lett.* **1984**, *177*, 287–290.
 (41) Elias, H.; Chou, M. H.; Winkler, J. R. *J. Am. Chem. Soc.* **1988**, *110*, 429–434.
 (42) Dixit, B. P. S. N.; Moy, V. T.; Vanderkooi, J. M. *Biochemistry* **1984**, *23*, 2103–2107.
 (43) Dixit, B. P. S. N.; Waring, A. J.; Vanderkooi, J. M. *FEBS Lett.* **1981**, *125*, 86–88.

- (44) Magner, E.; McLendon, G. *J. Phys. Chem.* **1989**, *93*, 7130–7134.
 (45) Qin, L.; Kostić, N. M. *Biochemistry* **1994**, *33*, 12592–12599.
 (46) Shen, C.; Kostić, N. M. *J. Electroanal. Chem.* **1997**, *438*, 61–65.
 (47) Shen, C.; Kostić, N. M. *Inorg. Chem.* **1996**, *35*, 2780–2784.
 (48) Hamachi, I.; Takashima, H.; Hu, Y. Z.; Shinkai, S.; Oishi, S. *Chem. Commun.* **2000**, 1127–1128.
 (49) Uhlenheuer, D. A.; Wasserberg, D.; Nguyen, H.; Zhang, L.; Blum, C.; Subramaniam, V.; Brunsveld, L. *Chem.-Eur. J.* **2009**, *15*, 8779–8790.
 (50) Zadnarm, R.; Schrader, T. *J. Am. Chem. Soc.* **2005**, *127*, 904–915.

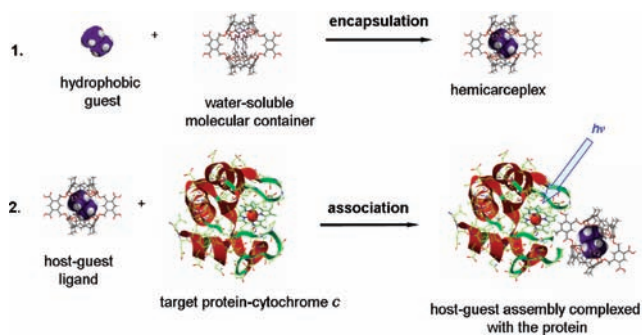


Figure 3. Schematic representation of (1) encapsulation of the guest molecule within the hydrophobic cavity of octacarboxyhemicarceand; and (2) binding of the complete hemicarceplex to the target protein.

concentration of the hemicarceplex was equilibrated with the zinc-substituted cytochrome *c*. The association between ZnCC and the encapsulated guest was probed by electron transfer quenching of the long-lived phosphorescence of $^3\text{ZnCC}^*$.

Materials. Horse heart Type III cytochrome *c*, anhydrous CoF_2 , zinc acetate, ferrocene (Fc), 1,1'-ferrocenedicarboxylic acid, 1,4,5,8-naphthalenetetracarboxylic acid, adamantane, benzoquinone, and chloranil were used without further purification. Duroquinone (DQ) was purified by sublimation and recrystallization. All chemicals were purchased from Sigma-Alfa. Ruthenocene was kindly provided by Prof. Frieder Jäkle. The octacarboxyhemicarceand was prepared following the published procedure.⁵¹ Anhydrous HF gas was obtained from Matheson Tri-Gas Inc.

Zinc-Substituted Cytochrome *c*. The first batch of zinc cytochrome *c* was prepared as described by Vanderkooi and Erecinska^{52,53} by the modified method of Flatmark and Robinson⁵⁴ and Fisher et al.⁵⁵ Later, this method was further optimized (see the Supporting Information). Protein solutions were prepared using 20 mM phosphate buffer (pH = 7–10) containing 0.1 M NaCl in 20% glycerol. Consistent with the established procedures, the purity of the protein was assessed by monitoring the A_{423}/A_{549} ratio in the UV–vis absorption spectrum. Only fractions with $A_{423}/A_{549} \geq 15.8$ were used (see the Supporting Information, Figure S2).

Guest Encapsulation and Binding to the Protein. The host–guest complex was prepared by adding the appropriate amount of the solid guest to aqueous, slightly basic solution of hemicarceand of known concentration (2×10^{-4} M, 5×10^{-5} M, 2×10^{-5} M) to obtain the final host–guest ratio of 1:1. The encapsulation time depended on the guest compound. The reaction was spectroscopically monitored for at least 24 h and allowed to fully equilibrate. The resulting mixture was filtered prior to mixing with an equal volume of the protein solution (for details, see the Supporting Information). The concentration of ZnCC was determined on the basis of the absorbance at 423 nm, $\epsilon = 243 \text{ mM}^{-1} \text{ cm}^{-1}$.⁵⁶

Photophysical Properties. Absorption spectra were recorded on a Cary 500 UV–vis NIR spectrometer. Emission spectra were measured on a Varian Cary Eclipse fluorescence spectrometer with excitation at 420 nm. Time-resolved phosphorescence experiments were carried out on the Varian Cary Eclipse or using a home-built

photon counting system, which employed either a Hamamatsu Xe flash lamp or a Cube 404 nm, 100 mW diode laser (Coherent) as the excitation source. The lamp provided $\sim 2 \mu\text{s}$ wide broadband pulses, which were filtered by a bandpass filter (427 nm, 10 ± 2 nm fwhm). The duration of the diode laser pulse was varied from 0.5 to 10 μs as needed. The emitted photons passed through a 550 nm long-pass filter and were detected by a cooled R928 Hamamatsu PMT and counted by an SR400 photon counter (SRS). The system was operated at 40 Hz repetition rate with the synchronization provided by a DG535 delay generator (SRS). The solutions for all phosphorescence measurements were exhaustively degassed by freeze–pump–thaw cycles until no change in the recorded lifetime was observed.

Data Analysis. Time-resolved measurements of Zn–cytochrome *c* emission show that the delayed fluorescence exhibits the same lifetime as the $^3\text{ZnCC}^*$ phosphorescence. Therefore, either phosphorescence or delayed fluorescence can be used to monitor the triplet lifetime. Because the phosphorescence quantum yield is low, it was more convenient and reliable to analyze data recorded at the delayed fluorescence wavelength. The decay of $^3\text{ZnCC}^*$ was not a pure single exponential, although it can be fit satisfactorily with a monoexponential function. Biexponential fitting revealed the presence of a minor, $\sim 10 \pm 2\%$ component with a considerably shorter lifetime, $\tau = 1.5 \pm 0.5$ ms, in all reference samples with and without the hemicarceand. Because the short-lived component accounts for only 10% of the overall phosphorescence amplitude, it was decided to analyze the kinetic data in terms of a single exponential function. The resulting error is minor. It should be clarified that the $\sim 10\%$ short-lived component in the transient is not synonymous with the presence of a 10% impurity in our protein samples. The fixed 404 nm wavelength of the diode laser lies closer to the absorption maximum of the free-base porphyrin (404 nm) rather than of the ZnCC (423 nm). As a result, the contribution of the residual free-base CC to the transient is greater than its content in the sample, which on the basis of the A_{423}/A_{549} ratio we estimate at no more than 2%. Throughout the photon counting experiments, the integrity of the protein was controlled by monitoring the A_{423}/A_{549} ratio in the UV–vis absorption spectrum. We did not observe any growth of absorption in the vicinity of 404 nm or spectral shifts, which would indicate leaching out of the zinc ion or other protein degradation.

Results

Association between Zn–Cytochrome *c* and the Empty Hemicarceand. Addition of the empty octacarboxyhemicarceand to the ZnCC solution induces changes in the position of the absorption and emission peaks, as well as in the radiative lifetime of the triplet state. These effects show that association between the supramolecular cage and the cytochrome takes place and leads to the modification of the photophysical properties of the latter. At 1×10^{-6} M cytochrome concentration and 1:1 hemicarceand: ZnCC ratio, an approximately 2 nm hypsochromic shift of the Soret band of ZnCC is observed. The shift reaches its maximum value of 5 nm at 30:1 cage:protein ratio (see the Supporting Information for the complete results of the titration experiments, Figure S3). Smaller, approximately 3 nm blue shifts in the fluorescence and phosphorescence spectra of ZnCC were also observed. Hypsochromic shifts in the absorption spectrum of native cytochrome *c* upon binding to liposomes and membranes were reported in the past.^{57,58} They were attributed to the alteration in the Zn–porphyrin environment brought about by the interaction of the protein with the acidic

(51) Piatnitski, E. L.; Flowers, R. A., II; Deshayes, K. *Chem.-Eur. J.* **2000**, *6*, 999–1006.

(52) Vanderkooi, J. M.; Erecinska, M. *Eur. J. Biochem.* **1975**, *60*, 199–207.

(53) Vanderkooi, J. M.; Adar, F.; Erecinska, M. *Eur. J. Biochem.* **1976**, *64*, 381–387.

(54) Flatmark, T.; Robinson, A. B. In *Structure and Function of Cytochromes*; Okunuki, K., Kamen, M. D., Sekuzu, I., Eds.; University Park Press: Baltimore, MD, 1968; pp 383–387.

(55) Fisher, W. R.; Taniuchi, H.; Anfinson, C. B. *J. Biol. Chem.* **1973**, *248*, 3188–3195.

(56) Ivković-Jensen, M. M.; Kostić, N. M. *Biochemistry* **1997**, *36*, 8135–8144.

(57) Tuominen, E. K. J.; Wallace, C. J. A.; Kinnunen, P. K. *J. Biol. Chem.* **2002**, *277*, 8822–8826.

(58) Nantes, I. L.; Zucchi, M. R.; Nascimento, O. R.; Faljoni-Alario, A. *J. Biol. Chem.* **2001**, *276*, 153–158.

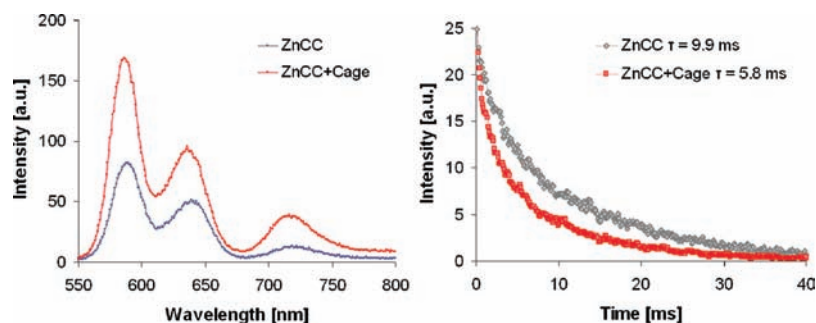


Figure 4. Phosphorescence spectra and normalized decay profiles of 1×10^{-6} M ZnCC in the absence and presence of 1×10^{-4} M of the empty hemicarcerand at pH = 7. The phosphorescence peak is at 720 nm, while the 584 and 635 nm peaks are due to delayed fluorescence.

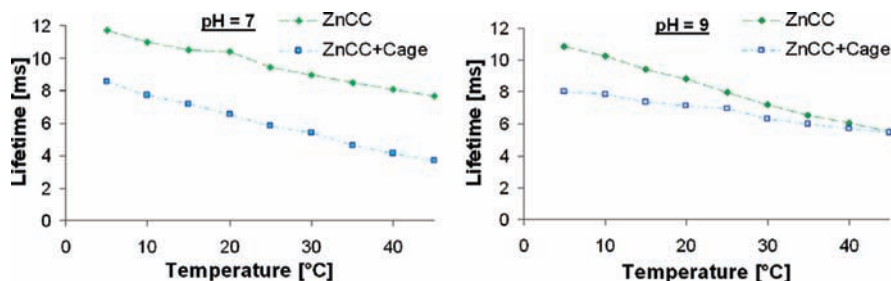


Figure 5. Temperature dependence of the triplet lifetime of ZnCC (1×10^{-6} M) in the absence and in the presence of the empty octacarboxyhemicarcerand (1×10^{-4} M) at pH = 7 and 9.

substrates. A blue shift of the phosphorescence maximum of ZnCC bound to cytochrome *c* peroxidase (CcP) was also reported.⁵⁹ It was explained in terms of the increased torsion of the porphyrin ring upon binding to the peroxidase.

No changes in the fluorescence intensity and lifetime of ZnCC in the presence of the empty hemicarcerand were detected. However, the behavior of the long-lived triplet state was significantly altered. A dramatic, more than 2-fold increase of phosphorescence intensity was observed upon binding of the hemicarcerand to the protein, with a parallel decrease in the triplet lifetime (Figure 4). It could be argued that the increased phosphorescence intensity is due to the protection from residual quenchers, for example, O_2 , offered by the bulky cage bound to the surface of the protein. However, if this were the case, a corresponding increase in the triplet state lifetime of cytochrome *c* would have to occur. This was not observed. On the contrary, the ZnCC triplet lifetime decreased from 9.9 ms in free solution to 5.8 ms in the presence of the cage. The simultaneous growth of emission intensity and the decrease of lifetime point to the increase of the T_1-S_0 transition moment and the corresponding acceleration of the radiative decay. The behavior of the T_1 state of zinc porphyrins is known to respond strongly to the distortions of the ring, as well as to small changes in the distance and orientation of the axial ligands, in this case the His18 residue.^{60,61} Both factors are influenced by binding. The observed lifetime and intensity changes are strong indications that the hemicarcerand binds to cytochrome *c* in the vicinity of the heme pocket and modulates the axial ligation of the Zn center. This behavior is distinct from the solvation effects reported by Winkler et al.⁶²

The influence of the hemicarcerand on the $^3\text{ZnCC}^*$ lifetime is most pronounced under neutral and slightly basic conditions. It diminishes at increasing pH and disappears altogether at pH = 10, indicating that the association of the supramolecular cage with cytochrome *c* is driven primarily by electrostatic interactions. Variable temperature measurements of the T_1 lifetime of ZnCC and ZnCC+Cage further underscored the strong pH dependence of the association between the cage and cytochrome *c*. As can be seen in Figure 5, the $^3\text{ZnCC}^*$ lifetime decreases with increasing temperature both in the presence and in the absence of the hemicarcerand. The $^3\text{ZnCC}^*$ and $^3\text{ZnCC}^*+\text{Cage}$ lifetimes give rise to distinct lines with slopes determined primarily by the thermal repopulation of the S_1 state, which is a significant triplet decay pathway in Zn-porphyrins. At neutral pH, the ZnCC+Cage complex remains stable over the entire 5–45 °C temperature range, as evidenced by the two distinct lines. At pH = 9, electrostatic attraction between the cage and ZnCC is greatly diminished. The complex is more labile, and at 45 °C the $^3\text{ZnCC}^*$ and $^3\text{ZnCC}^*+\text{Cage}$ lifetime traces coalesce, indicating that above that temperature, only one species, the free uncomplexed ZnCC, is present.

Importantly, spectral shifts and lifetime changes similar to these described above were not observed at any pH when small molecules bearing multiple carboxylic groups, for example, 1,4,5,8-tetracarboxynaphthalene, were added to the ZnCC solution. This suggests that the binding to cytochrome *c* depends not only on the acidity of the ligand, but also on its size, conformational flexibility, and ability to participate in multi-valent interactions.³⁶

Photoinduced Electron Transfer between Zn–Cytochrome *c* and Encapsulated Guests. Photoinduced electron transfer was used to probe the association between the supramolecular host–guest assembly and cytochrome *c* in more detail. Because $^3\text{ZnCC}^*$ can act as both an electron donor and acceptor depending on its redox partner, the same molecular container

(59) Koloczek, H.; Horie, T.; Yonetani, T.; Anni, H.; Maniara, G.; Vanderkooi, J. M. *Biochemistry* **1987**, *26*, 3142–3148.

(60) Hoffman, B. M. *J. Am. Chem. Soc.* **1975**, *97*, 1688–1694.

(61) Nappa, M.; Valentine, J. S. *J. Am. Chem. Soc.* **1978**, *100*, 5075–5080.

(62) Kim, J. E.; Pribisko, M. A.; Gray, H. B.; Winkler, J. R. *Inorg. Chem.* **2004**, *43*, 7953–7960.

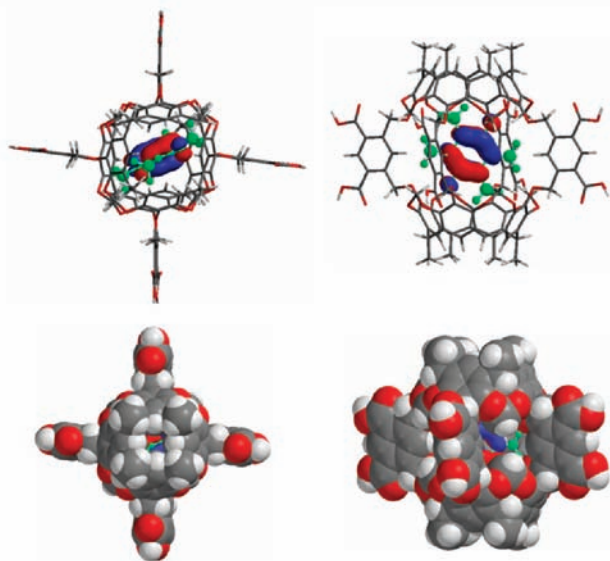
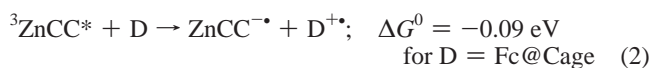
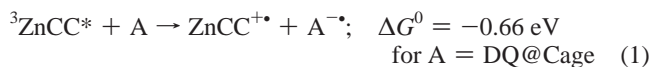


Figure 6. Duroquinone encapsulated within the octacarboxyhemicarcerand. The cage distorts slightly away from the ideal D_{4h} symmetry in the presence of the guest. The LUMO orbital of the host–guest complex is localized on duroquinone (AM1). The space-filled model shows that the encapsulated guest molecule cannot come into direct contact with the surface of the cytochrome.

could be used to transport reducing and oxidizing guest ligands and position them in the vicinity of the active site of the cytochrome. The oxidative (1) and reductive (2) ET reactions with the respective driving forces are shown below:



The choice of the guest molecules was dictated primarily by the size of the hemicarcerand cavity. Despite this constraint, we were able to include redox-active guests spanning a nearly 1 eV range of driving force (ferrocene, ruthenocene, and duroquinone), as well as adamantane and naphthalene, which are not capable of oxidizing or reducing ${}^3\text{ZnCC}^*$. The relevant molecular orbitals participating in the electron transfer reaction (LUMO of duroquinone and HOMO of ferrocene) are localized on the guest molecule and do not appreciably extend onto the hemicarcerand (Figure 6). As a result, the electron transfer reactions between the ZnCC and the redox-active guests satisfy the conditions of a weakly coupled process and can be analyzed in terms of the Marcus theory.

Hemicarceplexes studied in this work are thermodynamically stable in aqueous solution and do not rely on Cram's "constrictive binding". The affinity depends on the shape and the hydrophobicity of the guest. The driving force for the encapsulation by the water-soluble hemicarcerand and hence the stability of the host–guest complex can be predicted on the basis of the free energy change associated with the reduction of hydrophobic surface exposed to water. The 178 \AA^2 hydrophobic surface of ferrocene combined with Honig's $47 \text{ cal mol}^{-1} \text{ \AA}^{-2}$ hydrophobic energy⁶³ yields encapsulation free energy of

-8.4 kcal/mol . Similar treatment of the more polar duroquinone yields net stabilization energy of -5.6 kcal/mol . In this case, one has to account for the 2.9 kcal/mol loss of hydration energy of duroquinone (Spartan calculation). These estimates are remarkably close to the calorimetrically determined binding energies reported by Cram and Deshayes^{4,25,51} and provide useful guidance in the design of the encapsulation experiments. Encapsulation of guest molecules occurs spontaneously within minutes to hours, indicating the presence of an activation barrier associated with the ingress and egress from the cage.^{25,64} The incarceration kinetics depends on the size of the guest and its solubility in the aqueous medium. For example, the encapsulation of duroquinone, which is slightly soluble in water and whose shape facilitates the passage through the portal, is relatively rapid (Supporting Information, Figure S4). The encapsulation of the nearly insoluble ferrocene, ruthenocene, and adamantane was considerably slower and required overnight equilibration.

The interaction of the photoexcited Zn–cytochrome *c* with the encapsulated redox-active guests (ferrocene, ruthenocene, and duroquinone) results in efficient quenching of the triplet state of the former. The reduction of the phosphorescence intensity is accompanied by a corresponding decrease of the triplet state lifetime (Figure 7). The quenching rates follow the expected thermodynamic trend and increase as the ΔG^0_{ET} of the electron transfer reaction becomes more negative (Table 1). No quenching was observed in the presence of encapsulated naphthalene or adamantane, for both of which electron transfer to or from ${}^3\text{ZnCC}^*$ is strongly endothermic. Encapsulated ruthenocene, for which the electron transfer to ${}^3\text{ZnCC}^*$ is slightly endoergic, did cause phosphorescence quenching, albeit at rates approximately 10 times slower than the Fc@Cage (Figure 8, Table 1, and Supporting Information, Figure S5). To verify the primarily electrostatic nature of the association between the hemicarceplex and cytochrome *c*, experiments at different pH values were conducted (Supporting Information, Table S1). The efficiency of quenching by both Fc@Cage and Fc(COOH)₂ is diminished in increasingly basic solutions. At pH = 10, when approximately ~25% of the positive charges on the surface of cytochrome *c* are neutralized, the rate of the electron transfer quenching of ${}^3\text{ZnCC}^*$ by Fc@Cage reduced by a factor 3 in comparison with pH = 7. Remarkably, in all cases in which direct comparison is possible, ET rates observed for the redox-active host–guest complexes are considerably higher than these for the corresponding free acceptors and donors in solution. For example, the encapsulated duroquinone, DQ@Cage, quenches ${}^3\text{ZnCC}^*$ 20 times faster than free duroquinone (DQ) at a similar concentration. The reductive quenching of ${}^3\text{ZnCC}^*$ by Fc@Cage is 3 times faster than by the same concentration of free ferrocene dicarboxylic acid (Figure 7, Table 1). These results confirm that the hemicarceplex binds to cytochrome *c* and positions the redox active guest in the vicinity of the Zn-substituted heme. The difference between the free versus encapsulated quenching rates is larger in the case of DQ and DQ@Cage, because duroquinone is not likely to associate with cytochrome *c* as much as the ferrocene dicarboxylic acid does.

The concentration dependence of the ET quenching rate of ${}^3\text{ZnCC}^*$ by Fc@Cage and DQ@Cage is shown in Figure 9. The rates were measured in $2 \times 10^{-6} \text{ M}$ solutions of ZnCC in which the hemicarcerand guest ratio was always kept at 1:1

(63) Sharp, K. A.; Nicholls, A.; Fine, R. F.; Honig, B. *Science* **1991**, 252, 106–109.

(64) Pagba, C.; Zordan, G.; Galoppini, E.; Piatnitski, E. L.; Hore, S.; Deshayes, K.; Piotrowiak, P. *J. Am. Chem. Soc.* **2004**, 126, 9888–9889.

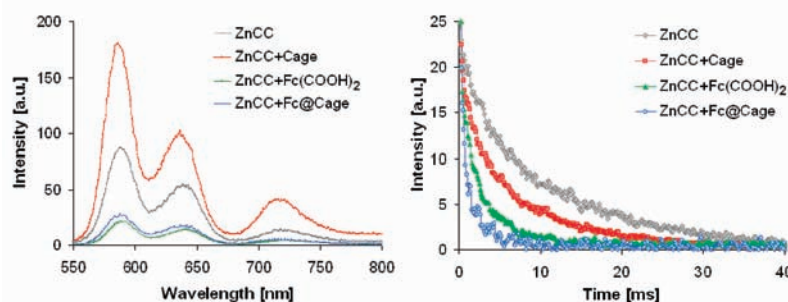


Figure 7. Phosphorescence spectra and emission decay profiles of 1×10^{-6} M ZnCC in the presence of the empty cage (1×10^{-4} M), encapsulated ferrocene (1×10^{-4} M), and ferrocene dicarboxylic acid (1×10^{-4} M) at pH = 7.

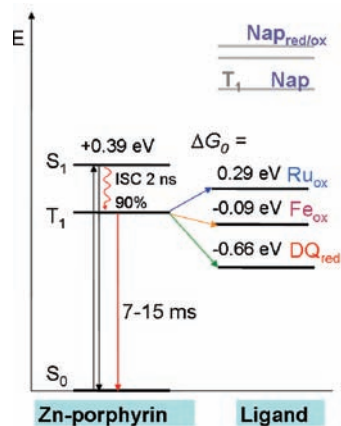


Figure 8. The free energy diagram for the reaction of $^3\text{ZnCC}^*$ with DQ@Cage, Fc@Cage, Ru@Cage, and the redox inactive Naph@Cage.

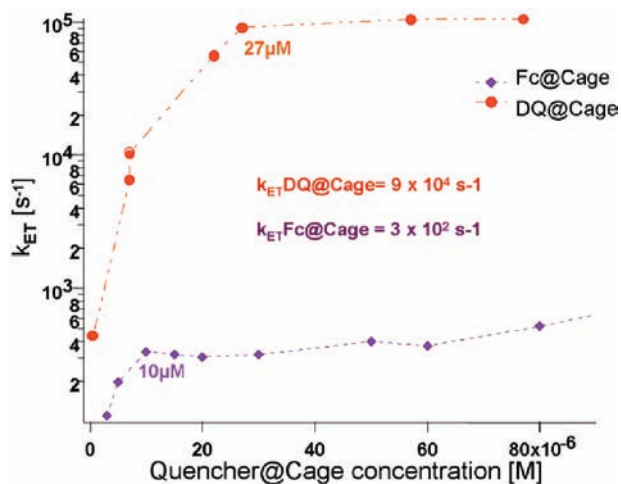


Figure 9. Concentration dependence of the electron transfer kinetics of $^3\text{ZnCC}^*$ (2×10^{-6} M) with Fc@Cage and DQ@Cage at pH = 7. The DQ@Cage trace has been corrected for the quenching by the free duroquinone, $k_{\text{DQ@Cage}} = k_{\text{measured}} - k_{\text{DQ}}$.

throughout the studied concentration range. Both traces in Figure 9 show the initial sharp increase of the quenching rate with the rising concentration of the quencher followed by a plateau. In both cases, the region of rate increase is steeper than it would have been in the case of a diffusion-controlled process, indicating that the hemicarceplex binds to the cytochrome. The presence of the plateau is a further confirmation of the protein–hemicarceplex complex formation. Electron transfer rates in the plateau region are approximately 25 times faster

for DQ@Cage than for Fc@Cage and are consistent with the much higher driving force for the former, $\Delta G^0 = -0.66$ eV, versus -0.09 eV. Increasing the concentration of the hemicarceplex beyond the onset of the plateau leads to only a slight further acceleration of the rate. This suggests that guest@Cage complexes continue to bind to cytochrome *c*, forming higher than 1:1 protein–hemicarceplex aggregates; however, the successive dockings occur further away from the heme site and make only a minor contribution to the overall quenching rate. It is significant that the DQ@Cage and Fc@Cage traces differ markedly from one another in the onset of the plateau. In the case of the incarcerated ferrocene, the leveling off occurs very early, at approximately $10 \mu\text{M}$, while for encapsulated duroquinone it takes place much later, at nearly $30 \mu\text{M}$. The divergence results from the different affinity of the hemicarceplex toward the hydrophobic, completely insoluble ferrocene and the comparatively polar and somewhat water-soluble duroquinone. The octacarboxyhemicarceplex traps ferrocene with a very high binding constant, $K_{\text{encaps}} > 10^8 \text{ M}^{-1}$. As a consequence, even at the lowest micromolar concentrations, ferrocene is present in solution exclusively in the encapsulated form. The saturation point of the Fc@Cage curve corresponds to the concentration at which the 1:(1:1) complex of cytochrome *c* with the Fc@Cage hemicarceplex is the predominant species. Therefore, this point can be used to estimate the binding constant between the hemicarceplex and the cytochrome, $K_{\text{assoc}} = 1 \times 10^5 \text{ M}^{-1}$. Similar affinity, $K_{\text{assoc}} = 2 \times 10^5 \text{ M}^{-1}$, was reported by Fisher et al. for the binding of tetracarboxyphenylporphyrin with the native cytochrome *c*.⁶⁵ Duroquinone is considerably more soluble in water than ferrocene. Absorbance measurements in the same buffer as used in the above experiments yielded a saturated concentration of free duroquinone of $2.3 \times 10^{-5} \text{ M}$ (Supporting Information, Figure S4). As a result, at low micromolar concentrations, the $\text{DQ} + \text{Cage} \rightleftharpoons \text{DQ@Cage}$ equilibrium favors free duroquinone and empty hemicarceplex. Indeed, the quenching rates obtained with duroquinone concentrations below $20 \mu\text{M}$ are similar regardless of whether the hemicarceplex is present in the solution or not. The DQ@Cage host–guest complex becomes the dominant form only at a concentration that is higher than that corresponding to the formation of a 1:1 hemicarceplex–ZnCC complex. As a consequence, for DQ@Cage, the onset of the plateau in Figure 9 signifies the point at which all hemicarceplexes bound to the surface of the protein become occupied by duroquinone. The duroquinone encapsulation constant estimated on this basis is $K_{\text{encaps}} \approx 4 \times 10^4 \text{ M}^{-1}$, with the corresponding free energy of

(65) Clark-Ferris, K. K.; Fisher, J. *J. Am. Chem. Soc.* **1985**, *107*, 5007–5008.

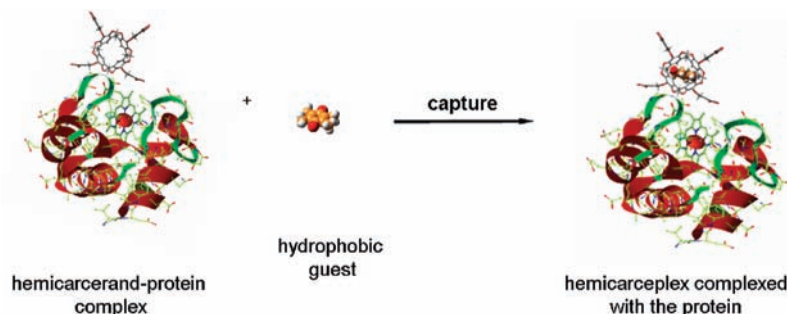


Figure 10. Capture of the guest by the octacarboxyhemicarcerand associated with cytochrome *c*.

6.3 kcal/mol. These results are close to the values of 1×10^4 M^{-1} and 5.6 kcal/mol predicted on the basis of the hydrophobic area and the hydration energy of duroquinone. This agreement supports the validity of the binding analysis. The encapsulation of 1,4-benzoquinone (BQ) and chloranil (CQ) is not complete in the investigated concentration range because of the higher solubility of these two compounds in water. For this reason, only the quenching rates by free benzoquinone and chloranil are reported in Table 1.

The Binding Region. The thermodynamic parameters and distance dependence of electron transfer can be used to estimate the separation between the donor and acceptor in a manner similar to FRET (Foerster resonance energy transfer).^{66,67} Naturally, such estimates are highly approximate and cannot pinpoint a specific binding site. Nevertheless, they can be used to identify the general binding region of the hemicarceplex on the surface of the cytochrome. While in FRET the rate decreases as R^{-6} and the relevant Franck–Condon factors are given by the overlap between the emission spectrum of the donor and the absorption spectrum of the acceptor, in electron transfer, the rate decays as $k = k_0 \cdot e^{-\beta R}$, with the slope β characteristic of the specific material. The ET Franck–Condon factors are estimated with the help of the classical Marcus equation⁶⁸ or its semiclassical variants.⁶⁹ The value of β has been determined for a variety of intervening media, including covalent linkers, SAMs, frozen glasses, and proteins. For the purpose of this approximation, we treat the protein and the wall of the cage as a homogeneous tunneling barrier with effective β of 1.1 \AA^{-1} . This attenuation factor was determined by Gray et al.⁷⁰ for Fe^{III} –cytochrome *c* with electron donors covalently attached to its surface. Because the electron transfer reactions between $^3\text{ZnCC}^*$ and ferrocene and duroquinone lie within the “normal” thermodynamic region, the classical Marcus equation can be used:

$$k(R_{\text{DA}}) = \left(\frac{\pi}{\hbar^2 \lambda k_{\text{B}} T} \right)^{1/2} \cdot |V|^2 \cdot \exp \left[-\frac{(\Delta G^0 + \lambda)^2}{4 \lambda k_{\text{B}} T} \right]$$

where $|V|^2 = |V_0|^2 e^{-\beta R_{\text{DA}}}$

The magnitude of the reorganization energy λ is a necessary parameter for the determination of the donor–acceptor separation. Our kinetic data yield $\lambda = 0.8$ eV (see the Supporting Information). As anticipated, this value is lower than most

reorganization energies reported for electron transfer between cytochrome *c* and redox partners exposed to the aqueous solution. Reorganization energies ranging from 0.8 to 1.5 eV were reported for ET reactions involving native FeCC.^{71,72} The retrieved value of λ is consistent with the reduced solvation of the redox center encapsulated within the hydrophobic cage. The Zn-to-Fe and Zn–DQ distance in the hemicarceplex–cytochrome complex calculated on the basis of $\beta = 1.1 \text{ \AA}^{-1}$ and $\lambda = 0.8$ eV is 16.5 \AA . This is a much shorter distance than the center-to-center separation in a random encounter complex between the hemicarceplex and the cytochrome, which is 22.1 \AA . The latter value would lead to 500 times slower ET rates than these observed experimentally. This suggests that the hemicarceplex has a preference for binding at the surface region proximal to the heme pocket, which is the ET pathway in the self-exchange reaction of cytochrome *c* and has been invoked in its interaction with several metal complexes,⁷³ the copper-containing plastocyanin,^{56,74} and cytochrome *b*₅.^{45,75}

Discussion

While we focused on demonstrating that the same hemicarcerand can deliver both reducing and oxidizing partners to the target protein, the reported results have broader implications for the design of supramolecular carrier molecules. The dynamic behavior of the hemicarcerand–guest–protein ternary assembly is determined by the relative host–guest and host–protein affinities. The long lifetime of the excited triplet state of ZnCC enabled us to investigate two distinct regimes: one of tight encapsulation and one of rapid guest exchange. In both cases, the role of the hemicarcerand is more complex than that of a conventional solubilizer or phase transfer catalyst. In the simpler to analyze tight encapsulation limit, $K_{\text{encaps}} \gg K_{\text{assoc}}$, the hemicarcerand transports the ligand to the desired target while protecting it from the aqueous medium. This case, in which the hemicarceplex behaves as a stable chemical species, is represented in Figure 3. On the other hand, if $K_{\text{assoc}} > K_{\text{encaps}}$, the host–guest complex is more labile than the complex between the hemicarcerand and the protein. In this regime, the cage docked to the surface of the protein acts as an artificial receptor, which intercepts the ligand from solution and positions it in the vicinity of the active site of cytochrome *c*. This situation,

(66) Scholes, G. D. *Annu. Rev. Phys. Chem.* **2003**, *54*, 57–87.

(67) Cristian, L.; Piotrowiak, P.; Farid, R. S. *J. Am. Chem. Soc.* **2003**, *125*, 11814–11815.

(68) Marcus, R. A. *J. Chem. Phys.* **1956**, *24*, 966–978.

(69) Jortner, J.; Bixon, M. *J. Chem. Phys.* **1988**, *88*, 167–170.

(70) Gray, H. B.; Winkler, J. R. *Proc. Natl. Acad. Sci. U.S.A.* **2005**, *102*, 3534–3539.

(71) Gray, H. B.; Winkler, J. R. *Annu. Rev. Biochem.* **1996**, *65*, 537–561.

(72) Ivković-Jensen, M. M.; Ullmann, G. M.; Young, S.; Hansson, Ö.; Crnogorac, M. M.; Ejdebäck, M.; Kostić, N. M. *Biochemistry* **1998**, *37*, 9557–9569.

(73) Marcus, R. A.; Sutin, N. *Biochim. Biophys. Acta* **1985**, *811*, 265–322.

(74) Zhou, J. S.; Kostić, N. M. *Biochemistry* **1992**, *31*, 7543–7550.

(75) McLendon, G. L.; Winkler, J. R.; Nocera, D. G.; Mauk, M. R.; Grant Mauk, A.; Gray, H. B. *J. Am. Chem. Soc.* **1985**, *107*, 739–740.

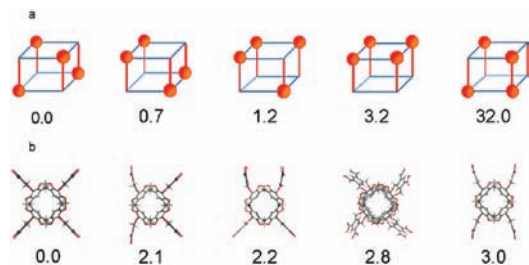


Figure 11. (a) Location of the negative charges and the relative relaxed energies of the distinct quadruply deprotonated forms of the octacarboxy-hemicarcerand (in kcal/mol, AM1 in vacuo). In the first four structures, only one carboxylic group per *m*-phthalic acid “portal” is charged. In the last structure, one of the portals is doubly deprotonated, giving rise to a sharp energy increase. (b) Examples of the distorted fully protonated hemicarcerand with corresponding energies relative to the D_{4h} minimum (in kcal/mol, AM1 in vacuo).

depicted in Figure 10, is more challenging from the kinetic point of view; however, it opens fascinating possibilities for the design of hybrid biosynthetic systems. For example, one can envision how suitably engineered host molecules could be used to selectively intercept substrates and increase the number of turnovers of a biocatalytic reaction. The tight encapsulation limit is relevant to transporting drugs and contrast agents and protecting them from the contact with the biological medium until they reach the selected target. The reversibility of the assembly disassembly process and its sensitivity to stimuli such as temperature and pH mimics the behavior of biological systems and allows for fine adjustments of the binding equilibria and kinetics.

A point that deserves some discussion is the high affinity of the hemicarcerand toward cytochrome *c* and its binding preference, which is different from that of small acidic ligands with similar pK_a values. This behavior stems from the ability of the hemicarcerand to adapt to the charge distribution and shape of the protein. Under the mildly basic conditions of our experiments, on the average one carboxylic group on each of the four *m*-phthalic acid portals of the cage exists in the ionic form. The possible distinct, not symmetry related locations of the four negative charges on the surface of the hemicarcerand are shown in Figure 11a. The calculated gas-phase energy differences between the unique arrangements are small, in part, because the flexible cage relaxes to accommodate multiple charges on its surface. The introduction of a second negative charge onto the same portal carries a much higher energetic penalty (the last entry in Figure 11a). Such higher energy forms may become important in interactions with sufficiently basic sites, but are of minor importance in the studied pH range. The existence of several nearly isoenergetic and readily interconverting charge distributions allows the hemicarcerand to match the surface electrostatics of its binding partner. The variety of charge distributions is augmented by the structural flexibility of the outer section of the hemicarcerand. Pivoting of the portals alters

the shape of the molecule at the expense of only a modest energy increase (Figure 11b). Distortions change the spacing between the carboxylic groups and expose the hydrophobic regions of the cage, enabling the hemicarcerand to better interact with the hydrophobic regions of the protein. Small, rigid ligands with similar pK_a values do not possess such electrostatic and conformational flexibility and for this reason exhibit a binding preference determined purely by the basicity of the available sites. This behavior is consistent with the findings of Jain et al. and points to the importance of multivalent interactions in the binding of large synthetic molecules with biological targets.³⁶ An important feature of the octacarboxy-hemicarcerand used in this study is the relative rigidity of its core, whose inner volume is independent of the position and ionization state of the portals. In this fashion, the encapsulation of the guest and the target binding functions are decoupled from one another.

Conclusions

A water-soluble hemicarcerand was used as a shuttle to dock structurally diverse reducing and oxidizing ligands to zinc-modified cytochrome *c*. To our knowledge, this is the first demonstration of bidirectional redox chemistry between a metalloprotein and supramolecular host–guest assembly. The association between the hemicarcerand and the protein, as well as the encapsulation of the guest, are reversible and can be controlled by varying the pH and temperature of the medium. Such capacity to undergo multiple self-assembly/disassembly cycles mimics the dynamic behavior of natural systems more closely than do hybrid constructs with permanently appended synthetic cofactors. The kinetic behavior of the ternary guest–hemicarcerand–protein assembly depends on the relative strength of the host–guest and host–protein interactions. The regime in which the reversibly docked supramolecular host acts as a selective artificial receptor and modulates the ligand–protein interaction is of particular interest and potential for inventive biomedical and biocatalytic applications.

Acknowledgment. C.V.P. and P.P. would like to thank Prof. Jane Vanderkooi for the kind demonstration of the cytochrome *c* metal exchange procedure. Partial support of this work by the Busch Biomedical Grant (P.P.) and U.S. DOE Grant DE-FG02-06ER15828 (P.P.) is gratefully acknowledged. K.I.J. acknowledges support through the Rutgers Dissertation Fellowship program.

Supporting Information Available: Optimized procedure for the metal exchange in cytochrome *c*, complete record of the titration of ZnCC with the empty octacarboxy–hemicarcerand, time-lapse of the encapsulation of duroquinone by the hemicarcerand, examples of the pH dependence of the ET quenching rate and examples of double exponential phosphorescence decay fits, and explanation of the data analysis. This material is available free of charge via the Internet at <http://pubs.acs.org>.

JA102188E